



**HAL**  
open science

## Lead(II) Formate in Rembrandt's Night Watch: Detection and Distribution from the Macro- to the Micro-scale

Victor Gonzalez, Ida Fazlic, Marine Cotte, Frederik Vanmeert, Arthur Gestels, Steven de Meyer, Frédérique Broers, Joen Hermans, Annelies van Loon, Koen Janssens, et al.

► **To cite this version:**

Victor Gonzalez, Ida Fazlic, Marine Cotte, Frederik Vanmeert, Arthur Gestels, et al.. Lead(II) Formate in Rembrandt's Night Watch: Detection and Distribution from the Macro- to the Micro-scale. *Angewandte Chemie International Edition*, 2023, 10.1002/anie.202216478 . hal-03969238

**HAL Id: hal-03969238**

**<https://hal.science/hal-03969238>**

Submitted on 20 Feb 2023

**HAL** is a multi-disciplinary open access archive for the deposit and dissemination of scientific research documents, whether they are published or not. The documents may come from teaching and research institutions in France or abroad, or from public or private research centers.

L'archive ouverte pluridisciplinaire **HAL**, est destinée au dépôt et à la diffusion de documents scientifiques de niveau recherche, publiés ou non, émanant des établissements d'enseignement et de recherche français ou étrangers, des laboratoires publics ou privés.

## Heritage Science

How to cite:

International Edition: doi.org/10.1002/anie.202216478

German Edition: doi.org/10.1002/ange.202216478

# Lead(II) Formate in Rembrandt's *Night Watch*: Detection and Distribution from the Macro- to the Micro-scale

Victor Gonzalez<sup>+</sup>,\* Ida Fazlic<sup>+</sup>, Marine Cotte<sup>+</sup>, Frederik Vanmeert, Arthur Gestels, Steven De Meyer, Frédérique Broers, Joen Hermans, Annelies van Loon, Koen Janssens, Petria Noble, and Katrien Keune

**Abstract:** *The Night Watch*, painted in 1642 and on view in the Rijksmuseum in Amsterdam, is considered Rembrandt's most famous work. X-ray powder diffraction (XRPD) mapping at multiple length scales revealed the unusual presence of lead(II) formate, Pb(HCOO)<sub>2</sub>, in several areas of the painting. Until now, this compound was never reported in historical oil paints. In order to get insights into this phenomenon, one possible chemical pathway was explored thanks to the preparation and micro-analysis of model oil paint media prepared by heating linseed oil and lead(II) oxide (PbO) drier as described in 17<sup>th</sup> century recipes. Synchrotron radiation based micro-XRPD (SR-μ-XRPD) and infrared microscopy were combined to identify and map at the micro-scale various neo-formed lead-based compounds in these model samples. Both lead(II) formate and lead(II) formate hydroxide Pb(HCOO)(OH) were detected and mapped, providing new clues regarding the reactivity of lead driers in oil matrices in historical paintings.

## Introduction

Rembrandt van Rijn (1606–1669) is one of the most innovative Dutch 17<sup>th</sup>-century painters. *The Night Watch*, painted in 1642, today displayed in the Rijksmuseum, Amsterdam, is one of his most important masterpieces. It is the largest extant work of art he ever painted, measuring 3.79 × 4.53 m. Rembrandt showcased his virtuosity, not only by achieving a bold composition with striking light and shadow effects, but also by his constant search for novelty in painting materials and techniques. In 2019, *Operation Night*

*Watch*, the largest research and conservation project ever undertaken for Rembrandt's masterpiece was initiated.<sup>[1]</sup> The research questions were threefold: i) How did Rembrandt paint *The Night Watch*? ii) What is the condition of the painting? iii) How can we best preserve it for future generations? These questions were addressed in a multidisciplinary manner in close collaboration with conservators, art historians and scientists. The materiality of the painting was chemically investigated using various complementary analytical techniques, in particular chemical imaging methods that operate at multiple length scales. Paintings are

[\*] Dr. V. Gonzalez<sup>+</sup>

Université Paris-Saclay, ENS Paris-Saclay, CNRS, PPSM  
 4 Av. des Sciences, 91190 Gif-sur-Yvette (France)  
 E-mail: victor.gonzalez@ens-paris-saclay.fr

Dr. V. Gonzalez,<sup>+</sup> I. Fazlic,<sup>+</sup> F. Broers, Dr. J. Hermans,  
 Dr. A. van Loon, P. Noble, Prof. K. Keune  
 Rijksmuseum Conservation & Science  
 Hobbemastraat 22, 1071 ZC Amsterdam (The Netherlands)

I. Fazlic<sup>+</sup>, Dr. M. Cotte<sup>+</sup>  
 ESRF, the European Synchrotron Radiation Facility  
 71 Avenue des Martyrs, 38000 Grenoble (France)

Dr. M. Cotte<sup>+</sup>  
 Laboratoire d'Archéologie Moléculaire et Structurale (LAMS),  
 Sorbonne Université, CNRS, UMR8220  
 4 place Jussieu, 75005 Paris (France)

Dr. F. Vanmeert, A. Gestels, S. De Meyer, F. Broers, Prof. K. Janssens  
 AXIS Antwerp X-ray Imaging and Spectroscopy laboratory, University of Antwerp  
 Groenenborgerlaan 171, 2020 Antwerp (Belgium)

Dr. F. Vanmeert  
 Paintings Laboratory, Royal Institute for Cultural Heritage (KIK-IRPA)  
 Jubelpark 1, 1000 Brussels (Belgium)

F. Broers, Dr. J. Hermans, Prof. K. Keune

Van't Hoff Institute for Molecular Sciences, University of Amsterdam  
 Science Park 904, 1090 GD Amsterdam (The Netherlands)

F. Broers  
 Inorganic Chemistry & Catalysis, Debye Institute for Nanomaterials  
 Science & Institute for Sustainable and Circular Chemistry, Utrecht  
 University  
 Universiteitsweg 99, 3584 CG Utrecht (The Netherlands)

A. Gestels  
 InViLab UAntwerp Industrial Vision Lab, University of Antwerp  
 Groenenborgerlaan 171, 2020 Antwerp (Belgium)

[\*] These authors contributed equally to this work.

© 2023 The Authors. Angewandte Chemie International Edition published by Wiley-VCH GmbH. This is an open access article under the terms of the Creative Commons Attribution Non-Commercial NoDerivs License, which permits use and distribution in any medium, provided the original work is properly cited, the use is non-commercial and no modifications or adaptations are made.

highly heterogeneous materials, both along the surface of the painting and in depth (from varnish to support). Accordingly, the composition and the distribution of materials were determined from the macro-scale -via large maps acquired directly on *The Night Watch*- to the micro-scale -via various (sub)microscopic modalities on minute samples taken from the artwork. This helps assessing the original paint components, conservation and degradation products, and the painting technique. In this research, our attention is focused on the identification and mapping of the various lead compounds. Lead-based pigments have been abundantly used by Rembrandt in his paintings,<sup>[2]</sup> the most common form being lead white (LW), a synthesized pigment typically containing lead carbonates, hydrocerussite  $\text{Pb}_3(\text{CO}_3)_2(\text{OH})_2$  (HCer) and cerussite  $\text{PbCO}_3$  (Cer, Table S1). Besides LW, lead can also be found in other pigments (e.g. lead-tin yellow  $\text{Pb}_2\text{SnO}_4$ , LTY), in drying agents (lead(II) oxide  $\text{PbO}$ , red lead or minium,  $\text{Pb}_3\text{O}_4$ ) or in degradation products (e.g. lead sulfates, notably palmierite,  $\text{K}_2\text{Pb}(\text{SO}_4)_2$ , the latest being extensively present in *The Night Watch*). X-ray powder diffraction (XRPD) techniques have proven to be highly efficient to simultaneously detect and discriminate these various lead compounds, and were applied both at the macro-scale via macro-XRPD (MA-XRPD) and at the micro-scale via SR- $\mu$ -XRPD.<sup>[3]</sup> This study reports on the detection of the very unusual compound lead(II) formate,  $\text{Pb}(\text{HCOO})_2$  (LF) in the paint layers of *The Night Watch*, and discusses its specific distribution from the macro- to micro-scale. This, together with a study of mock-ups, allows us to propose hypotheses regarding the origin of this unusual compound.

## Results and Discussion

### Analysis of *The Night Watch*

In total, about  $0.55 \text{ m}^2$  of the painting surface (corresponding to 26 small area maps) were scanned using a MA-XRPD prototype laboratory instrument.<sup>[4]</sup> Briefly, the X-ray beam ( $\text{Cu K}\alpha$  anode, ca.  $140 \mu\text{m}$  diameter X-ray source spot) impinged on the painting under an angle of  $10^\circ$ . XRPD patterns were collected in reflection geometry by raster scanning the surface of the painting. In this case, the painting remained stationary while the X-ray instrument performed the scanning movements (details in Supporting Information). Unsurprisingly, HCer and Cer were identified in many parts of the painting. Much more remarkably, LF was occasionally detected by MA-XRPD. Careful assessment of the 26 collected MA-XRPD maps revealed its presence in 12 maps. As illustrated in Figure 1 and detailed in Table S2, some trends can be observed:

- LF is systematically found in light-coloured, LW-rich (and in one case also containing LTY) areas of the painting (Figure 1).
- In 10 of the 12 maps, plumbonacrite (PN),  $\text{Pb}_5(\text{CO}_3)_3\text{O}(\text{OH})_2$ , another relatively rare lead carbonate, is also found co-localized with LF (Figure 1). PN was previously identified in other Rembrandt's paintings, in LW *impasto*

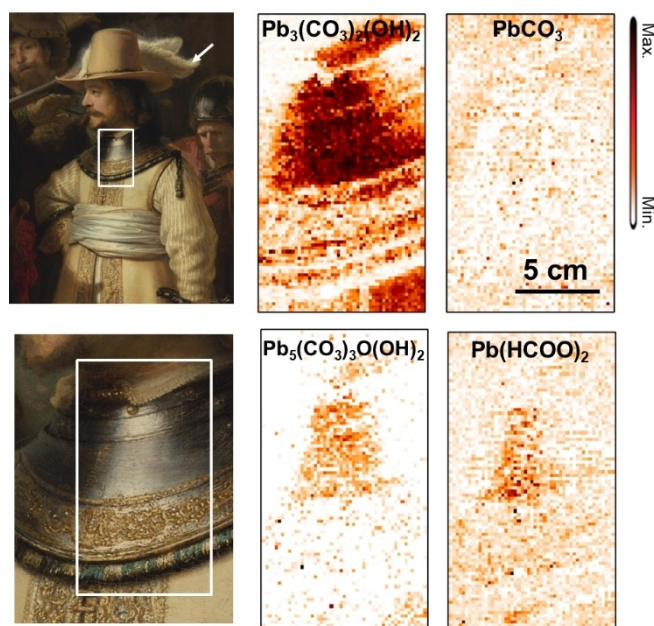


**Figure 1.** MA-XRPD crystalline phases distribution on the area of the steel gorget of Willem van Ruytenburch on *The Night Watch* (1642) by Rembrandt van Rijn (1606–1669). White rectangles indicate the area scanned using MA-XRPD. The white arrow indicates the location of sample SK-C-5\_1457.

areas (thickly applied paint with a clear three-dimensional morphology).<sup>[3b]</sup>

- HCer is always present in the regions where LF and PN are detected. In some regions (e.g. Figure 1), HCer is mainly in LF regions; in other regions (see Table S2), HCer is more concentrated outside LF regions.
- In the latter regions, HCer is usually associated with Cer. Cer is less concentrated in the LF regions (Figure 1).

MA-XRPD maps of LF are often noisy (Figure 1 and Figure S1), because of their low detected intensity, in particular when compared to the HCer map in Figure 1. To confirm the presence of LF in *The Night Watch*, and gain insight into its distribution at the micro-scale, SR- $\mu$ -XRPD mapping was performed on paint micro-fragments. During *Operation Night Watch*, about 50 paint samples were taken to address different research questions. Maps were acquired in transmission geometry by raster scanning of the resin-embedded cross-sections in front of a micrometric X-ray beam (see details in Supporting Information).<sup>[5]</sup> LF was detected in three of these paint cross-sections. One of these samples (SK-C-5\_070), was purposely taken from a LF-rich area as identified by MA-XRPD, in the girl's light yellow dress (Figure S1D14).

Sample SK-C-5\_070 (Figure 2A) shows a LTY+LW layer (as shown by the distribution of LTY, cassetite  $\text{SnO}_2$  and HCer). The near absence of Cer (only a few grains visible), combined with the detection of PN throughout the paint layer suggest that a non-standard LW is present here. In addition, a  $\approx 80 \mu\text{m}$  diameter lead soap protrusion (a globular lump that has formed *in situ* in the paint layers)<sup>[6]</sup> is

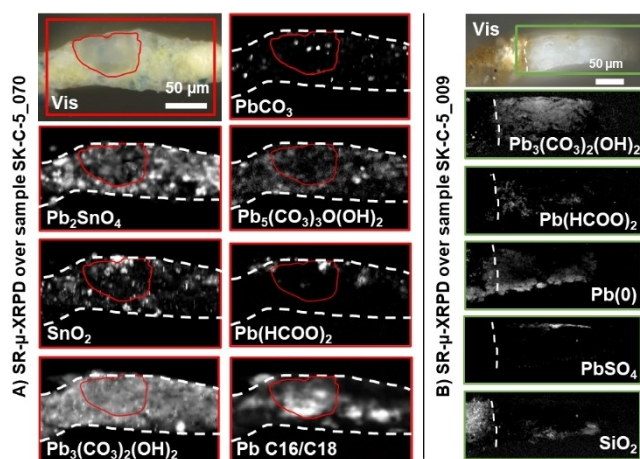


**Figure 2.** SR- $\mu$ -XRPD crystalline phases distribution on samples A) SK-C-5\_070 from the girl's light yellow dress (the circular red shape indicates the protrusion) and B) SK-C-5\_009 (the white dotted line represents the interface between the protrusion and the ground layer). The red and green rectangles indicate the area scanned on each sample. The intensities scale from min (black) to max (white).

visible in the middle of the map (red circular shape), in which crystalline mixed lead soaps (identified as approximately a mixture of palmitate/stearate soaps with a 1:1 ratio through their peaks at  $1.28$ ,  $2.62$  and  $3.93 \text{ nm}^{-1}$ )<sup>[7]</sup> were found. Interestingly, HCeR diffraction signals were broader in the protrusion than in the surrounding LW layer (full-width at half maximum (FWHM) of peak HCeR (012) of  $0.16^\circ$  and  $0.11^\circ$  respectively as measured with the ID13 setup, Figure S2). This suggests that part of the HCeR was formed or re-crystallized *in situ* in the protrusion. LF was detected near the top surface of the paint, mainly inside but also outside the protrusion.

Sample SK-C-5\_009 (Figure 2B) shows part of a protrusion that formed within the clay-based ground - the preparatory layer that was used by Rembrandt for *The Night Watch*. The sample was taken in a degraded area from the dog in the lower right of the painting (Figure S3). In this region, no Pb-compounds could be observed above the detection limits of MA-XRPD. However, with SR- $\mu$ -XRPD, LF was found throughout the protrusion. HCeR is homogeneously present in the protrusion, while no CeR was detected. A thin layer of anglesite ( $\text{PbSO}_4$ ), a degradation compound<sup>[8]</sup> was detected at the surface of the sample. Surprisingly, metallic lead was also detected throughout the map that we interpret as the result of SR beam-induced alteration of LF as observed by following the evolution of the diffraction intensities under repeated acquisitions (Figure S4). Indeed, we have recently reported the formation of  $\text{Pb}^0$  in LW-based paint layers under high-intensity X-ray beams.<sup>[5a]</sup> Even more recently, the formation of  $\text{Pb}^0$  from LF solutions upon electron beam irradiation was described<sup>[9]</sup> possibly opening up future lines of enquiry about the treatment of heavy metals-contaminated water. Here again, the FWHM of HCeR (012) estimated on the P06 data was broader ( $0.16^\circ$ ) than the one of the original HCeR pigment ( $0.06^\circ$ ) measured on another sample not shown here.

Sample SK-C-5\_1457 was taken from an *impasto* area (feather of the hat of lieutenant Willem van Ruytenburch) (Figure S5). The paint layer is homogeneously white and mostly contains HCeR and some CeR. Both PN and LF are present (mainly in the lower part of the section), but not colocalized at the micro-scale (Figure S5).

In addition, micro-Fourier transform infrared spectroscopy in attenuated total reflectance mode ( $\mu$ -FTIR-ATR) maps were acquired on the first two samples, to evaluate its potential as an alternative technique to SR- $\mu$ -XRPD to detect and map LF and to gain complementary molecular characterization (technical details available in Supporting Information). The formal identification of LF is made very difficult by the overlapping signals of other lead carboxylates and lead carbonates. However, in the central part of the protrusion of SK-C-5\_009, the average FTIR spectrum shows a signal compatible with the presence of LF<sup>[10]</sup> (Figure S6).

Results obtained with SR- $\mu$ -XRPD confirm some of the trends observed with MA-XRPD: when LF is detected, this is in the light-coloured or white areas; PN and HCeR are present as well, but these three lead phases are not colocalised at the micro-scale; CeR always shows a lower amount, when detected at all. In two of the three samples, LF is detected in a protrusion, in addition to the surrounding paint.

The fact that MA-XRPD and SR- $\mu$ -XRPD did not systematically detect the same phases in the same area, (e.g. sample SK-C-5\_009), can be ascribed to the different instrumental configurations (in addition of the beam size, X-ray energy and corresponding penetration depth ( $\approx 10 \mu\text{m}$  in a LW layer in the MA-XRPD configuration), source intensity, detector, geometry), leading to different limits of detection, to the intrinsic heterogeneity of paint at both scales, and the limited representativity of few  $\approx 300 \mu\text{m}$  samples in a  $> 15 \text{ m}^2$  painting.

To our knowledge, this is the first report of the presence of LF in an historical painting. There are few occurrences of metal formates in cultural heritage materials, most often associated with degradation of glass, calcareous materials, cements and sandstones, or metals and alloys.<sup>[11]</sup> Concerning historical paintings, only zinc formate has been reported so far: in Jack Chambers' *Summer Visitor*<sup>[12]</sup> and in Salvador Dalí's *Couple with Clouds in their Heads*, where zinc formate dihydrate ( $\text{Zn}(\text{HCOO})_2 \cdot 2\text{H}_2\text{O}$ ) was found associated with  $\text{Zn}(\text{CH}_3\text{COO})_2 \cdot 2\text{H}_2\text{O}$  and  $\text{ZnS}$ .<sup>[12]</sup> In both cases, authors proposed that zinc formate was a degradation product of zinc white ( $\text{ZnO}$ ), possibly reacting with formic acid ( $\text{HCOOH}$ ) produced by the alkyd medium<sup>[12]</sup> or from the wooden frame.<sup>[13]</sup> So far, lead formate has only (recently) been reported in model paints, forming at the end of oxidative polymerization of model paint films prepared by mixing red lead ( $\text{Pb}_3\text{O}_4$ ) and four common drying oils (linseed, walnut, poppy-seed and stand oil).<sup>[14]</sup> In brief, in these studies by Švarcová et al., LF was detected within one day, by transmission XRPD but not in reflection geometry.  $^{13}\text{C}$ ,  $^1\text{H}$  and  $^{207}\text{Pb}$  solid state nuclear magnetic resonance spectroscopy confirmed the formation of LF. However, bulk FTIR (in transmittance mode on thin paints applied on



aluminium-coated glass slides) failed to detect them, which was ascribed to the overlap of the most intense IR peak of LF at  $1537\text{ cm}^{-1}$  [ $\nu_4$  asym. C–O stretch]<sup>[10a]</sup> with signals from oil and metal soaps.  $\text{Pb}^{\text{II}}$  (from  $\text{Pb}_3\text{O}_4$ ) reacts with oil, while the local chemical environment of  $\text{Pb}^{\text{IV}}$  atoms was found intact. The formation of formic acid in oils was also proven by gas chromatography-mass spectrometry, and LF was shown to form on  $\text{Pb}_3\text{O}_4$  powder exposed to volatile formic acid released during the autoxidation of oils, demonstrating the crucial role of oxygen in the process. Reactions crucial for the formation of formic acid, and subsequently LF, are the formation and decomposition of unsaturated ester hydroperoxides as primary oxidation products. Decomposition of hydroperoxides leads to the formation of secondary oxidation products, such as aldehydes, which further decompose to formic acid. A detailed chemical mechanism for the formation of formic acid and LF was proposed in the literature.<sup>[14a]</sup> Among the different oils tested, linseed oil is the most reactive towards the formation of LF, which would be due to its three isolated double bonds and their position near the methyl end in  $\alpha$ -linolenic acid.<sup>[14a]</sup> The scarcity of LF in historical paintings made Švarcová et al. suggest that these formate salts would not be stable and would only be an intermediate compound in the conversion of  $\text{Pb}_3\text{O}_4$  to lead soaps and/or lead carbonates. Therefore, the presence of LF in a 380-years-old painting calls for a reconsideration of this hypothesis. Also, beyond LF, there is an on-going controversy about the effect(s) (positive or negative) of lead carboxylates in general in paintings.<sup>[15]</sup> Lead carboxylates are involved in many degradation processes but they also play a major role in the rheological and drying properties of oil paints. Consequently, a better understanding of the possible origins of LF is highly desirable. It not only offers clues on painters' techniques and materials but also guides conservators towards developing better treatment methods for the preservation of artworks.

### Study of model samples

To explore a possible scenario for the presence of LF in *The Night Watch* we investigated a series of model samples, representative of historical paint layers, made with linseed oil (LO), the most common organic binder used in the 17<sup>th</sup> century. The occurrence of PN, stable only in alkaline conditions ( $\text{pH} > 10$ ), as well as the presence of newly formed HCer, led us to further explore the interactions of LO with lead(II) oxide ( $\text{PbO}$ ), an alkaline lead compound frequently used by 17<sup>th</sup>-century Dutch artists as an oil siccativ.<sup>[3b]</sup> Model “cooked oils” were prepared following the “huile de litharge” recipe reported by Turquet De Mayerne in 1633.<sup>[15]</sup> This recipe describes mixing and heating of oil and  $\text{PbO}$  (4:1 w/w) and adding hot water to the reacting mixture. In our model, 12 g of linseed oil (Kremer pigmente 73020) was cooked with 2.25 g (i.e. 75 % of the recipe 4:1 weight ratio) of  $\text{PbO}$  (Alfa Aesar, 99.9 %, 23 w % litharge,  $\alpha$ - $\text{PbO}$ , 77 w % massicot,  $\beta$ - $\text{PbO}$ ) for 3 h at  $100^\circ\text{C}$ , with or without 12 g of water (named PaWet and PaDry, respectively). The linseed oil was also heated with-

out  $\text{PbO}$  and water for comparison (LO). As previously discussed, such preparations result in the saponification of oil triglycerides and the formation of lead soaps (complexes of lead and fatty acids; in the case of LO, mainly triply unsaturated  $\alpha$ -linolenic acid, saturated palmitic and stearic acid, monounsaturated oleic acid and doubly unsaturated linoleic acid). This reaction is favored by the introduction of water.<sup>[16a]</sup> To simulate an incomplete dissolution/reaction of  $\text{PbO}$  as described in some historical texts, additional  $\text{PbO}$  particles (0.75 g per 4 g of heated medium, i.e. the remaining 25 % of the 4:1 weight ratio) were added and lightly mixed at room temperature (RT) to the cooked media (noted PaWetPbO and PaDryPbO), leading to the formation of large globules within the oil matrix (Figure 3). The appearance of these globules spans from orange to white and sometimes translucent when observed as a thin section (Figure 4). Finally, additional samples mimicking LW paints were prepared by mixing the above media (without and with the additional 25 % of  $\text{PbO}$ ) with LW (Kremer, HCer: Cer ratio of 90:10 w %, noted with the suffix LW). The list of model samples relevant to this work is presented in Table S3. The different model paints were spread on glass slides and left to dry for 3 years at RT. The optical microscope (OM) observation of the paint films revealed the formation of crystals from the first days of curing.

The precise kinetics of the formation of LF crystals will be the subject of a dedicated publication. The discussion here focuses on the macro- and micro-localization of crystals (see details in Table S3). Interestingly, a highly heterogeneous distribution of crystals was observed, with crystals (sometimes as needles  $> 100\ \mu\text{m}$ , Figure 4A and Figure S7A,B) strongly concentrated in thick regions and absent in the edges of the PaWet and PaDry films (Figure 3, Figure S8A, Figure S8B). These crystals were identified as LF thanks to SR- $\mu$ -XRPD (Figure 3, Figure 4A, Figure 4C, Figure S7A, Figure S7B, Figure S8A). It is noteworthy that

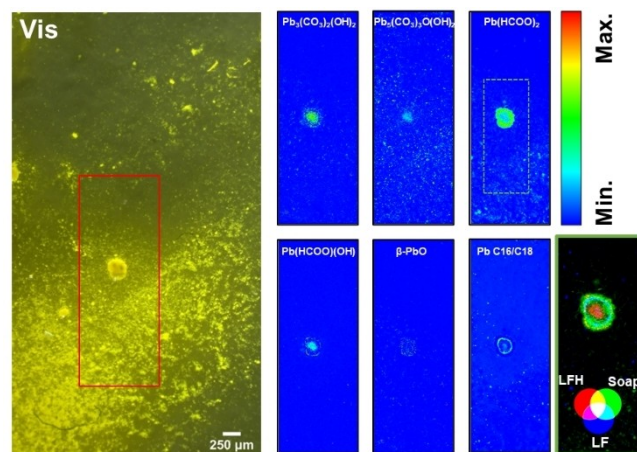


**Figure 3.** SR- $\mu$ -XRPD crystalline phases distribution on sample PaDryPbO, droplet laid on a glass slide. The red rectangle indicates the area scanned via SR- $\mu$ -XRPD, around a globule. In the bottom right corner, the RGB composite map displays a zoom around the globule (highlighted by the dotted green rectangle on LF map), with LFH (red), Pb C16 / C18 soaps (green) and LF (blue).

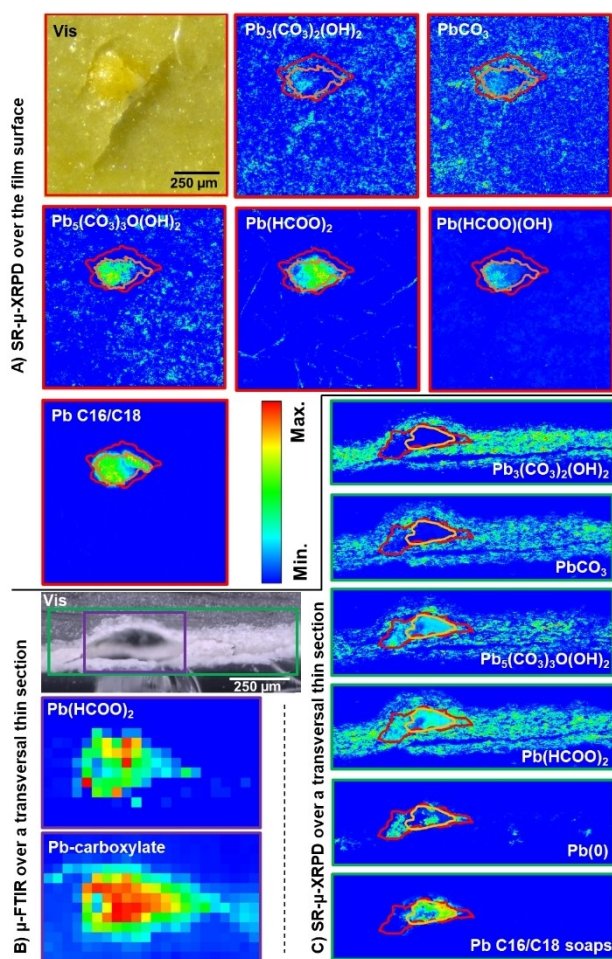


**Figure 4.** SR- $\mu$ -XRPD crystalline phases distribution and  $\mu$ -FTIR molecular groups distribution around a lead soap globule, in sample PaWetPbO\_LW. A) SR- $\mu$ -XRPD map over the film surface (red square); B), C) Maps over a thin section (resin embedded). Purple rectangle:  $\mu$ -FTIR; green rectangle: SR- $\mu$ -XRPD. The  $\mu$ -FTIR distributions were calculated by integrating the signal of the [ $\nu_5$  in-plane C–H bend] band ( $1365\text{--}1385\text{ cm}^{-1}$ ) for the LF; and of the [ $\nu$  asym. C–O stretch] band ( $1502\text{--}1564\text{ cm}^{-1}$ ) for the lead carboxylates. In A) and C), the color lines have been added to ease the comparison between the maps.

during the first SR- $\mu$ -XRPD experiments (at high dose) the transformation of LF into metallic lead was observed with Pb<sup>0</sup> colocalized with the LF crystals (Figure S7B). From then on, low X-ray dose conditions were favored to mitigate the reduction of lead(II).<sup>[5a]</sup> Small ( $<1\ \mu\text{m}$ ) PN particles were also detected in the paint media (Figure 3, Figure 4A, Table S3). In samples where LW was not added, small particles of newly formed HCer were sometimes detected, usually more concentrated in LF rich regions (Figure 3, Table S3). In these cases, Cer was not detected. In the samples prepared with LW pigment, LF crystals were not visible under the OM but could be clearly identified with SR- $\mu$ -XRPD (e.g. Figure 4A).

To assess the depth distribution of LF crystals in the models, transversal thin sections ( $5\text{--}10\ \mu\text{m}$ ) of cured films were prepared (Table S4). OM and SR- $\mu$ -XRPD highlighted

in most cases a lower concentration of crystals in the upper part ( $50\ \mu\text{m}$ ) of the cross-sections (Figure S7B). This observation could explain why Švarcová et al. observed LF with XRPD in transmission mode but not in reflection and supports their hypothesis of the influence of particle sedimentation on the distribution of LF. The  $\mu$ -FTIR map acquired on a thin section of cured PaDry succeeded in the detection of LF crystals, after non-negative matrix approximation calculations using the PyMCA ROI imaging software package<sup>[17]</sup> (Figure S7C).

To further assess the relationship between the paint film thickness and the LF distribution, additional PaDry and PaWet films of controlled thickness ( $15, 30, 60$  and  $90\ \mu\text{m}$ ) were prepared using a paint applicator. Thin sections ( $10\ \mu\text{m}$ ) of these samples were analyzed with SR- $\mu$ -XRPD after four months of natural aging. LF was not detected in this case (not shown). In addition, PaDry films of variable thickness were prepared using microscope glass slides with concave depression (Figure S10A). They revealed the absence of LF crystals in the thinner regions (Figure S10B, Figure S10C and Figure S10D). This result may explain why Švarcová et al. did not detect LF with FTIR spectroscopy. Based on our above observations, it is probable that in such thin layers, LF did not form. In our work, ATR-FTIR spectroscopy of thick ( $>0.3\ \text{mm}$ ) drops of PaDry was successful in the detection of LF, upon curing (Figure S9C).

A further complexity and heterogeneity of the system is reached when introducing additional PbO particles to the prepared cooked oil. 2D SR- $\mu$ -XRPD maps were acquired over the formed globules, both over the films surface (Figure 3, Figure 4A and Figure S11), and over thin-sections (Figure 4C). When mapped over the films surface, the globules usually present a complex onion-like structure with different Pb-based products distributed as successive layers. The composition of these core/shell structures varies from one sample to another and from one globule to another (Table S3). However, some trends can be observed and are illustrated with maps acquired on sample PaDryPbO (Figure 3) and PaWetPbO\_LW (Figure 4). PbO, when detected, was present at the core of the globule (Figure 3). The internal parts of the layered spheres (mixed with or just around the PbO core region) often contained a mixture of newly formed PN, HCer and in some cases, lead formate hydroxide Pb(HCOO)(OH) (LFH, Figure 3 and Figure S12B). LF was usually more concentrated in the second layer of the spherical mass (Figure 3 and Figure S12A), together or surrounded by other lead carboxylates. In some cases, mixed lead soaps (palmitate/stearate) were sufficiently crystallized to be firmly identified (Figure 3, Figure S12C).

A thin section ( $5\ \mu\text{m}$ ) was prepared from one of these lead soap globules (sample PaWetPbO\_LW) (Figure 4B and Figure 4C). SR- $\mu$ -XRPD maps show that in this globule, PbO has fully reacted away; the core of the globule contained crystallized mixed lead soaps, similar to *The Night Watch* sample SK-C-5\_070 (Figure 4C). LF and Pb<sup>0</sup> were colocalized around the core of the globule, forming the first onion-like layer (Figure 4C). Unlike in the PaDry and PaWet samples, LF was detected all over the film depth, including the upper parts. HCer, Cer, and PN (Figure 4C)



were found, spreading from the edge of the globule throughout the paint matrix. Previously observed LFH was not detected in this map, demonstrating a high heterogeneity and variability of the composition of these paints. In this thin section, LF was also detected with  $\mu$ -FTIR mapping (Figure 4B).

To investigate the direct reaction of PbO with oil, a simplified model system was prepared, consisting of cooked LO spread as a film on glass slides, and to which additional PbO particles were deposited (LO\_PbO). Two films were left to cure, at RT and at 60°C. This second sample was analyzed after 45 days and reanalyzed 2 years after the synthesis (after a first year at 60°C and a second year at RT) (Figure S11). LF, LFH and PN were all detected in the vicinity of PbO, successfully demonstrating that these compounds can form following the direct reaction of PbO with the oil. Finally, even though the long-term stability of LF will be the subject of a future publication, it should be noted that LF crystals were still present in paint films aged for three years at ambient conditions, and after two days of immersion of oil film (PaDry) samples in water.

Results obtained on the model paints can be summarized as follows:

- LF crystals formed during the curing of films of oil cooked with PbO (in both wet and dry conditions), sometimes in the form of needles up to  $\approx 100\ \mu\text{m}$  in length.
- In LW-free samples, LF concentration decreased with film depth and film thickness, leading to extremely heterogeneous systems and the absence of LF in some parts of the paint layer.
- LF was more concentrated around unreacted PbO particles, in the three systems (PaWet, PaDry, LO), and can also be present in an alkaline form: LFH (detected only in the \_PbO samples).
- LF (and its reduced  $\text{Pb}^0$  form) was detected in a lead soap-rich globule (protrusion) prepared as a thin section.
- Newly formed PN and HCer were detected both throughout the paint films and in the vicinity of the unreacted PbO particles.
- In addition to the lead soaps formed during the synthesis of the cooked oils, some additional soaps sometimes formed at RT and organized themselves as crystalline phases around PbO particles.

Figure 5 proposes two schemes to explain some of our findings on the model systems. The symbols used in the sketches follow the description of lead ionomer by Hermans et al.<sup>[18]</sup> Figure 5A is a model for the distribution of LF in curing oil films, while Figure 5B describes the more complicated case of the additional presence of unreacted PbO particles in the medium. In Figure 5A, LF is proposed to form from the substitution of formic acid (formed during oxidative curing of oil<sup>[14a]</sup>) with the different lead carboxylate groups: those formed during the preparation of the lead medium by saponification of oil triglycerides; but also those formed during the oil autoxidative drying, and the radical polymerization reactions.<sup>[18]</sup> Two hypotheses can explain the depth profile of LF crystals and their absence in thin films:

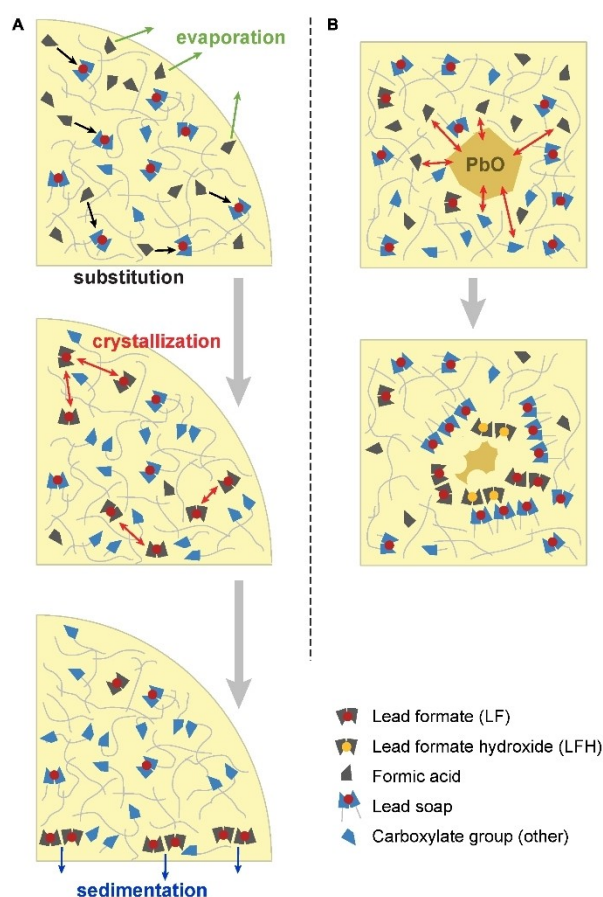


**Figure 5.** Schematic of the chemical and physical processes proposed to explain the micro- and macro-distribution of LF in paints. See text for the details. A) Model for the distribution of LF in PaDry and PaWet samples, cross-section of a paint droplet. Green, black, red and blue arrows represent evaporation of formic acid, substitution of formic acid on lead carboxylates, crystallization and sedimentation of LF, respectively. B) model for the distribution of LF and LFH in PaDry\_PbO, PaWet\_PbO and LO\_PbO samples, top view of PbO particles deposited in a paint film. Formic acids and mobile fatty acids migrate, react at the surface of PbO forming LFH, LF, lead soaps, and crystallize. For simplification and readability: i) the additional carbonates (PN, HCer...) phases are not represented; ii) possible additional pigments are not represented; iii) to facilitate reading, different colors are used for the different lead-based compounds (PbO, LF, LFH, lead carboxylates); iv) Inter conversion of LFH into LF, lead soaps into LF, LF and LFH into carbonates is not represented. The presence of hybrid lead oxide/hydroxide/formate/long chain carboxylate species cannot be excluded.

- 1) the evaporation of formic acid, in particular in thin paint layers or close to the paint surface (top part of Figure 5A);
- 2) the diffusion of small molecules of LF, assembling into crystals (middle part of Figure 5A), and sedimenting (bottom part of Figure 5A) in a less dense paint liquid film, further increasing the abundance of LF crystals at the bottom of the layer. While this sedimentation could have an influence on the distribution of LF in the oil matrix (as visible in samples PaWet and PaDry), it probably does not occur when the medium is mixed with LW pigment, as then, the paint matrix density strongly increases (as in sample PaWetPbO\_LW).

In the case of unreacted PbO particles, a secondary local source of Pb<sup>II</sup> ions is present in addition to lead soaps (Figure 5B). In such a case, our models show that an additional, more alkaline form of LF (LFH) can be observed. PbO particles react with formic acid and mobile fatty acids, leading to the local formation and crystallization of LFH, LF and additional lead soaps. The higher alkalinity closer to the center of the PbO particles could explain the distribution of LFH with respect to LF, as observed in Figure 3. In parallel to the formation of LF, LFH and lead soaps, PbO can also convert into PN and HCer by taking up CO<sub>2</sub> and water, explaining the detection of these different components in the paint film and the complex layered structure in the globules. Besides, conversion of one compound into another, for example LFH into LF, lead soaps into LF, LF or LFH into HCer cannot be excluded.<sup>[19]</sup>

An interesting question is still whether the simultaneous observation of LF, LFH, PN, HCer and lead soaps in similar regions means that (1) the heterogeneity of the system at the nano- to micro-scale translates into local variations of the thermodynamically favorable conditions for crystallization of the various phases; (2) our analyses reflect the composition of the system at a certain time, but do not account for its final, stable conditions. The kinetics of the formation of LF and associated compounds and their evolution under different environmental conditions and/or conservation treatments will be discussed in a dedicated publication.

Besides, when LW is added as a pigment, it may provide an additional source of Pb<sup>II</sup> for the formation of LF, further increasing the complexity and heterogeneity of the system. Additional samples containing LW as a single source of Pb<sup>II</sup> ions are under analysis.

## Conclusion

In conclusion, the results obtained on mock-up paints shed new light on the presence and distribution of LF in *The Night Watch*, and the possible reasons for their presence in oil paintings in general. In addition to Pb<sub>3</sub>O<sub>4</sub>, as studied by Švarcová et al., PbO can also lead to the fast formation of LF in paints, together with LFH, lead soaps, PN and HCer. Even if no crystalline PbO phases were detected in *The Night Watch*, and its use as a drier remains hypothetical, the presence and distribution of LF, PN and of newly formed HCer together with the local absence of Cer at both the macro- and micro-scales, as well as the presence of lead fatty carboxylates-rich protrusions support the hypothesis that the oil used for light-toned parts of the painting was treated by an alkaline lead drier. In both *The Night Watch* and the model samples, the distribution of LF crystals at the macro- and micro-scale is highly variable. This distribution can be related to the paint thickness and the presence of a local high concentration of alkaline Pb-species (as simulated with unreacted PbO in model samples) and the competing formation and possible inter-conversion of LF, LFH, lead soaps and lead carbonates. In the case of *The Night Watch*, an additional degree of complexity is added by the fact that

the painting has been (re)varnished in the past with an oil-based varnish. In 1756, Van Dijk published a booklet on the paintings in the Amsterdam Town Hall in which he wrote that he removed 'layers of boiled oil and varnish' from *The Night Watch*.<sup>[20]</sup> Boiled oil was usually prepared with a drier such as PbO. However, Van Dijk's identification of "boiled oil" is only based on his empirical findings during his cleaning and restoration of the painting. Another unknown is to what extent this revarnishing was conducted locally or on the entire paint surface. It may have provided a fresh source of formic acid causing different LF-rich areas to form in the painting in different periods. In particular, the LF present at the surface of sample SK-C-5\_070 might be linked to a reaction between formic acid from this varnish and the LW paint. Additional model samples will be prepared to assess this hypothesis. Lastly, a possible environmental origin of formic acid cannot be excluded, as observed in the corrosion of many metallic artifacts.<sup>[11]</sup>

Finally, even if LF, as a pure compound, is highly soluble in water ( $K_p \approx 2.9 \times 10^{-5}$ ), the paint matrix seems to protect it from the environment. Accordingly, LF, LFH and other metal formates such as zinc formate, may be detected in many more historical paintings in the future, if more attention is paid to these particular short chain lead carboxylates. However, it should be noted that their detection is challenging. First, the MA-XRPD set-up is only sensitive to surface compounds (up to 10 μm in LW paint) and our models show a lower concentration of LF at the paint film surface. Second, μ-FTIR, a technique widely available for the study of paint cross-sections, is not suited for the detection of LF in lead soap/lead carbonate matrices. SR-μ-XRPD is therefore highly recommended to track LF in fragments from historical paintings, while being careful to use as low an X-ray dose as possible. The formation of lead carboxylates with long fatty acid chains has received a lot of scientific interest;<sup>[15]</sup> in the light of this work, it will be very important to pay similar attention to the presence of shorter lead carboxylates as they can provide essential information about a painting's history and its conservation state. While until now metal formates have been mainly associated with corrosion and degradation products,<sup>[11]</sup> it will be interesting to see if LF plays any role (positive or negative) in the stability and optical properties of oil paintings.

## Acknowledgements

The authors thank the entire *Operation Night Watch* Team at the Rijksmuseum for their help during MA-XRPD measurements, their expertise and constant support, particularly E. Van Duijn for her precious insights regarding the painting's conservation history, as well as A. Krekeler and N. de Keyser for their help with taking and preparing *The Night Watch* samples. We thank M. Burghammer (ID13, ESRF) J. Garrevoet (P06, DESY), K. Ignatiev (I18, DLS) and N. Salvado (Universitat Politècnica de Catalunya) for their support during the synchrotron experiments. We are indebted to W. De Nolf (ESRF) for help with the processing of SR data. We thank S. Švarcová at the ALMA laboratory



(Institute of Inorganic Chemistry of the Czech Academy of Sciences) for providing us with a reference LF powder and for fruitful discussions. IF thanks J. Flapper (AkzoNobel) and B. de Bruin (UvA) for their follow-up of the work. VG and IF have received funding from the European Union's Horizon 2020 research and innovation programme under the Marie Skłodowska-Curie actions (Grant Agreement #945298-ParisRegionFP and COFUND Programme "InnovaXN" #847439 respectively). This research was partially funded by the "3D understanding of degradation products in paintings" (3D2P) project supported by the Netherlands Institute for Conservation, Art and Science (NICAS) and the Dutch Research Council (NWO) (project number 628.007.031). The ESRF beamtime was granted through the peer-reviewed BAG proposal HG-172 at ID13. The Historical materials BAG has been implemented with support from the European Union's Horizon 2020 research and innovation programme under grant agreement No 870313, Streamline. Beamtime at DESY was granted at P06 through proposals N° I-20190926 EC and I-20200185 EC. Parts of this research have been supported by the project CALIPSO-plus under the Grant Agreement 730872 from the EU Framework Programme for Research and Innovation HORIZON 2020. The collaboration between French and Dutch institutes has been and is supported by the Royal Netherlands Academy of Arts and Sciences, KNAW (Descartes-Huygens price 2018), and the PHC van Gogh granted by the French Ministries of European and Foreign Affairs, and of Higher Education, Research and Innovation. FWO (Brussels) is acknowledged for financial support under grant G054719N as well as Interreg Vlaanderen-Nederland via project Smart\*Light and BELSPO (Brussels) for the FEDtWIN mandate Macro-Imaging. The main partner of *Operation Night Watch* is AkzoNobel. *Operation Night Watch* is made possible by The Bennink Foundation, C. L. de Carvalho-Heineken, PACCAR Foundation, Piet van der Slikke & Sandra Swelheim, American Express Foundation, Familie De Rooij, Het AutoBinck Fonds, TBRM Engineering Solutions, Dina & Kjell Johnsen, Familie D. Ermia, Familie M. van Poecke, Bruker Nano Analytics, Henry M. Holterman Fonds, Irma Theodora Fonds, Luca Fonds, Piekden Hartog Fonds, Stichting Zabawas, Cevat Fonds, Johanna Kast-Michel Fonds, Marjorie & Jeffrey A. Rosen, Stichting Thurkow fonds, het Nachtwacht Fonds, Familie Van Ogtrop Fonds, Gemeente Amsterdam and the Amsterdam Museum. The authors are extremely grateful to the two anonymous reviewers for their invaluable comments and suggestions.

### Conflict of Interest

The authors declare no conflict of interest.

### Data Availability Statement

The data that support the findings of this study are available from the corresponding author upon reasonable request.

**Keywords:** Carboxylates · Lead Formate · Pigments · Rembrandt · X-Ray Diffraction

- [1] <https://www.rijksmuseum.nl/en/whats-on/exhibitions/operation-night-watch>.
- [2] D. Bomford, J. Kirby, A. Roy, A. Rüger, R. White, *Art in the making: Rembrandt*, Yale University Press, Yale, **2006**.
- [3] a) V. Gonzalez, M. Cotte, F. Vanmeert, W. de Nolf, K. Janssens, *Chem. Eur. J.* **2020**, *26*, 1703–1719; b) V. Gonzalez, M. Cotte, G. Wallez, A. van Loon, W. de Nolf, M. Eveno, K. Keune, P. Noble, J. Dik, *Angew. Chem. Int. Ed.* **2019**, *58*, 5619–5622; *Angew. Chem.* **2019**, *131*, 5675–5678.
- [4] S. De Meyer, F. Vanmeert, P. Storme, K. Janssens, *Painting as a Story 6th Interdisciplinary ALMA Conference*, Acta Artis Academica, Brno, **2017**, pp. 29–38.
- [5] a) M. Cotte, V. Gonzalez, F. Vanmeert, L. Monico, C. Dejoie, M. Burghammer, L. Huder, W. de Nolf, S. Fisher, I. Fazlic, N. Chauffeton, G. Wallez, N. Jiménez, F. Albert-Tortosa, N. Salvadó, E. Possenti, C. Colombo, M. Ghirardello, D. Comelli, E. Avranovich Clerici, R. Vivani, A. Romani, C. Costantino, K. Janssens, Y. Taniguchi, J. McCarthy, H. Reichert, J. Susini, *Molecules* **2022**, *27*, 1997; b) C. G. Schroer, P. Boye, J. M. Feldkamp, J. Patommel, D. Samberg, A. Schropp, A. Schwab, S. Stephan, G. Falkenberg, G. Wellenreuther, *Nucl. Instrum. Methods Phys. Res. Sect. A* **2010**, *616*, 93–97.
- [6] M. Cotte, E. Checroun, J. Susini, P. Walter, *Appl. Phys. A* **2007**, *89*, 841–848.
- [7] E. Kočí, J. Rohlíček, L. Kobera, J. Plocek, S. Švarcová, P. Bezdička, *Dalton Trans.* **2019**, *48*, 12531–12540.
- [8] V. Gonzalez, A. van Loon, S. W. Price, P. Noble, K. Keune, *J. Anal. At. Spectrom.* **2020**, *35*, 2267–2273.
- [9] E. Gliozzo, C. Ionescu, *Archaeol. Anthropol. Sci.* **2022**, *14*, 17.
- [10] a) C. J. H. Schutte, K. Buijs, *Spectrochim. Acta* **1964**, *20*, 187–195; b) P. Baraldi, *Spectrochim. Acta Part A* **1981**, *37*, 99–102.
- [11] G. Eggert, A. Fischer, *Heritage Sci.* **2021**, *9*, 26.
- [12] K. Helwig, M.-E. Thibeault, J. Poulin, *Stud. Conserv.* **2013**, *58*, 226–244.
- [13] K. Keune, G. Boevé-Jones, *Issues in contemporary oil paint*, Springer, Cham, **2014**, pp. 283–294.
- [14] a) S. Švarcová, E. Kočí, P. Bezdička, S. Garrappa, L. Kobera, J. Plocek, J. Brus, M. Šťastný, D. Hradil, *Dalton Trans.* **2020**, *49*, 5044–5054; b) S. Garrappa, E. Kočí, S. Švarcová, P. Bezdička, D. Hradil, *Microchem. J.* **2020**, *156*, 104842.
- [15] M. Cotte, E. Checroun, W. De Nolf, Y. Taniguchi, L. De Viguerie, M. Burghammer, P. Walter, C. Rivard, M. Salomé, K. Janssens, J. Susini, *Stud. Conserv.* **2017**, *62*, 2–23.
- [16] a) M. Cotte, E. Checroun, J. Susini, P. Dumas, P. Tchoreloff, M. Besnard, P. Walter, *Talanta* **2006**, *70*, 1136–1142; b) L. de Viguerie, P. A. Payard, E. Portero, P. Walter, M. Cotte, *Prog. Org. Coat.* **2016**, *93*, 46–60.
- [17] M. Cotte, T. Fabris, G. Agostini, D. Motta Meira, L. De Viguerie, V. A. Solé, *Anal. Chem.* **2016**, *88*, 6154–6160.
- [18] J. J. Hermans, K. Keune, A. Van Loon, P. D. Iedema, *Metal Soaps in Art*, Springer, Cham, **2019**, pp. 47–67.
- [19] M. R. Raychaudhuri, P. Brimblecombe, *Stud. Conserv.* **2000**, *45*, 226–232.
- [20] J. van Dijk, *Kunst en historiekundige beschrijving en aanmerkingen over alle de schilderyen op het stadhuis te Amsterdam*, Pieter Yver, Amsterdam, **1758**.

Manuscript received: November 8, 2022

Accepted manuscript online: January 2, 2023

Version of record online: ■■■, ■■■

## Research Articles

## Heritage Science

V. Gonzalez,\* I. Fazlic, M. Cotte,  
F. Vanmeert, A. Gestels, S. De Meyer,  
F. Broers, J. Hermans, A. van Loon,  
K. Janssens, P. Noble,  
K. Keune \_\_\_\_\_ e202216478

Lead(II) Formate in Rembrandt's *Night Watch*: Detection and Distribution from the Macro- to the Micro-scale



X-ray powder diffraction mapping at multiple length scales revealed the unusual presence of lead(II) formate,  $\text{Pb}(\text{HCOO})_2$ , in several areas of *The Night Watch*, Rembrandt's most famous painting. A possible chemical pathway resulting in the formation of this compound in historical oil paint was explored via micro-analysis, notably using synchrotron radiation. New clues on the reactivity of metallic driers in oil systems were thus gathered.